

# Advances in Physical Performances of UPE/ESOA Partially Bio-nanocomposites Reinforced with Graphene Nanoplatelets

<sup>1</sup>Shivkumari Panda, <sup>2</sup>Dibakar Behera, <sup>3</sup>Prasant Rath, <sup>4</sup>Tapan Kumar Bastia

<sup>1,2,3,4</sup> School of Applied Sciences (Chemistry), KIIT University, Bhubaneswar, Odisha, 751024, India

Corresponding Author: Shivkumari Panda

**Abstract:** - This paper reports successful fabrication and study of various properties of a unique blend based nanocomposite containing Unsaturated polyester (UPE) /Epoxidized soybean oil Acrylate (ESOA) resin(80:20w/w) with varying content of graphene nanoplatelets (GNPs) as the reinforcing filler. The composite was prepared by a novel technique with the use of a high intensity ultrasonicator and then hot press casting method. Three different specimens of UPE/ESOA nanocomposites were fabricated with addition of 1, 3 and 5 wt% of GNPs. 3wt% nanofiller loading showed superior essential characteristics and after that the properties reduced may be due to the nucleating tendency of the nanofiller particles. UPE/ESOA reinforced with GNPs resulted in an enhancement of properties. Also the XRD pattern showed the compatibility of the GNPs by introducing a peak around  $27^{\circ}$  in the nanocomposites. FTIR spectroscopy and SEM Properties are also in agreement with the compatibility. Nanocomposite with 3wt% GNPs also showed remarkable enhancement in mechanical, dynamic mechanical, thermal and electrical properties with successful enhancement in  $T_g$  corroborated from DSC analysis owing to the homogeneous distribution of nanofiller in the blend. So by introduction of a small quantity of graphene nanoplatelets endow the new class of multiphase nanocomposites with inimitable structure and unexpected broaden applicability.

**Keywords:-** UPE/ESOA blend, partially bio-nanocomposite, GNPs, XRD,  $T_g$  .

## I. INTRODUCTION

Carbon the 6th element in the periodic tables has always remained a fascinating material to the researcher and technologist. Diamond, graphite, fullerenes, carbon nanotubes and now newly discovered graphene are the most studied allotropes of the carbon family [1]. Graphene nanoplatelets (GNPs) are the advanced type of reinforcing filler materials with improved characteristics and high applicability. Producing high-purity and large amounts of GNPs has a high cost. Again the issues associated to their stability during the process of fabricating nano composite materials, researchers have recommended for using them in a pristine state, i.e., not to be handled as a functional group [2]. Currently the synthesis of blends and composites from renewable resources has turn into hottest research topic. This is due to the growing demand for eco-friendly sustainable materials and to reduce global warming by replacing petroleum-based resins with bio-based

ones. However, it is difficult to fully replace the traditional petroleum based polymeric materials by those from renewable resources mainly due to their poorer mechanical and thermo-physical properties in comparison with conventional petroleum-based polymers that are intended to be replaced. Again functionalized plant oils, when cured alone or even with styrene as reactive co monomer, yield rubberlike materials [3-6]. Thus, they need to be combined with such petroleum-based resins which can show high stiffness, strength and  $T_g$  owing to their chemical build-up and tightly cross linked structure. In this context, plant oils, such as soybean oil are being widely used for the “greening” of thermoset such as unsaturated polyester (UPE) which is well suited, as it contains stiff aromatic units. ESOA, a biodegradable resin synthesized from the reaction of acrylic acid with epoxidized soybean oil [7], is an attractive bio-resin for blending with UPE [8] because it is inexpensive with good properties and high applicability and can be “genetically engineered” for polymer-related applications. There are studies in which GNPs were used as fillers to enhance the properties of the epoxy matrix [9,10]. The new generation of hybrid composite materials with versatile mechanical, thermal and electrical properties are of particular interest to researchers [11, 12].

The principal concern of this paper was to study the effect of graphene nanoplatelets on the electrical, thermal and mechanical properties of the UPE/ESOA hybrid composite. The important contribution of this study is the successful fabrication of a hybrid matrix nanocomposites material of partially biodegradable thermoset resins reinforced with the GNPs filler. The nanocomposites specimens fabricated at a low cost evidenced high mechanical strength, good stability, making them suitable for applications in the manufacturing of components for various thermal and electrical applications.

## II. EXPERIMENTAL DETAILS

### 2.1 Materials:

Isophthalic polyester (Unsaturated polyester-UPE) was used as the resin (supplied by Vasavi Bala Resins, VBR-4301 and viscosity – 0.3P a.s). The ESOA was synthesized by using the reported method [8] in our laboratory from ESO. Methyl ethyl

ketone peroxide (MEKP) and cobalt naphthanate were used as catalyst and accelerator for unsaturated polyester and ESOA blend which were purchased from Sigma Aldrich. All chemicals and solvents were used without any purification. The graphene nanoplatelets (GNPs) used in this study were purchased from sigma Aldrich with an average plate diameter in the range of 1 to 2  $\mu\text{m}$ .

### 2.2 Method of Preparation of nanocomposite:

First of all blend of UPE/ESOA (80:20) was prepared by using our previously reported technique [8]. Then nanocomposites were prepared by introducing varying content of GNPs (1, 3, 5 wt %) into the blend. They were mixed thoroughly with a magnetic stirrer for about 1 hour at a temperature of 60°C. Then it was placed in an ultrasonicator at a high intensity for 2 hour. After that the mixture was leave for cooling.

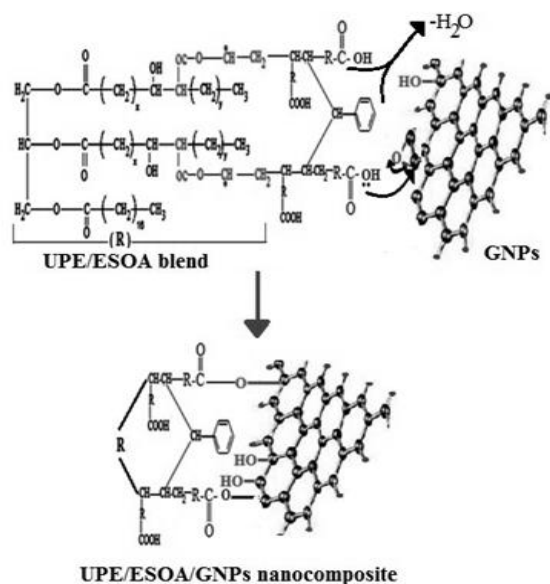


Fig.1: schematic diagram of reaction mechanism of UPE/ESOA/ GNPs nanocomposite.

Now, 5 % cobalt naphthanate (w/w) accelerator and then 3% MEKP (w/w) Catalyst was mixed with the above mixture and stirred for 15 min. After the catalyst was completely dissolved, the whole mixture was poured into the mould. At the beginning of fabrication, gel coat was uniformly brushed in to the finished side of male and female parts of the mould. Then the mould was subjected to hot-press (5 tons).Curing was carried out at 120°C in a convention oven for 2hour. Fig.-1 provides the schematic depiction of the possibility of chemical reaction taking place through the curing of the nanocomposite formed.

## III. INSTRUMENTS AND MEASUREMENTS

### 3.1 X-ray Diffraction (XRD):

The samples were subjected to X-ray diffraction (XRD-PW 1700, Philips, USA) using a filtered monochromatic radiation

of  $\text{CoK}_\alpha$  or  $\text{CuK}_\alpha$  of wavelength=0.17902 or 0.15420 nm through a Ni filter. The datas were collected with a computer, at a scanning speed of 0.05°/sec interfaced through the diffractometer. Datas were recorded in  $2\theta$  range of 2°–10° at the scan rate of 2°/min.

### 3.2 Fourier transforms infrared (FTIR) spectroscopy:

FTIR spectra of graphene nano platelets and UPE/ESOA/graphene nanocomposites were collected using Thermo-Nicolate Model 400 instrument equipped with a controlled temperature cell (Model HT-32 heated demountable cell used with an Omega 9000-A temperature controller).

### 3.3 Mechanical testing:

The tensile and flexural properties of different blends were studied by universal testing machine (HOUNSFIELD; H10KS) in accordance with ASTM D-638 and ASTM D-790. Impact strength was measured as per ASTM D256. All the results were taken as an average of four samples.

### 3.4 Scanning electron microscopy (SEM):

SEM was performed to qualitatively examine the surface morphology of the UPE/ESOA/Graphene nano platelets (GNPs) nano composite for varying content of the GNPs. The samples were gold coated and examined using a Philips 420T scanning electron microscope with a secondary electron detector, operating at 20 KV in the SEM mode.

### 3.5 Dynamic mechanical analysis (DMA):

For dynamic mechanical analysis, test specimens (56 x 13 x 3 mm) were cut from the center section of an ASTM Type I tensile bar. The dynamic mechanical properties like storage modulus and damping coefficient ( $\tan \delta$ ) were evaluated using a DMA tester (Model Q800).

3.6 *Differential Scanning Calorimetry (DSC):* DSC was utilized to find out the glass transition temperatures and to monitor the curing reactions. DSC was conducted on a Perkin Elmer Series 7 thermal analyzer under a nitrogen purge at a heating rate of 10° C/min. All reported data are from second heating scans.

### 3.7 Surface resistivity:

The surface resistivity of the nanocomposites having dimensions 100×100×3 mm was measured by using electrometer model 6517Keithley instrument according to ASTM D 257-2007. The resistivity was calculated at an electrification time of 60secs with applied voltage of 500 V DC.

### 3.8 Dry arc resistance:

Dry arc resistance of the test specimen (100×100×3 mm ) was conducted by using the arc resistance IEC model 2 instrument according to ASTM D 495-1999. The samples were located under the electrodes of space 6 mm and consisted of seven cycles. An arc is created between these electrodes and the

samples were exposed to it with low down voltage and elevated current condition.

### 3.9 Comparative tracking index:

The comparative tracking index (CTI) of the sample (3mm thickness) was calculated according to IEC 60 112-2003 under a voltage of 600-700 V and two electrodes resting on it with a load of 1 N. Drops of 0.1% Ammonium chloride electrolyte solution continually fall on the surface of sample in every 30 Sec until tracking occurs. The surface breakdown may take place from increased degradation of the insulating surface by minute localized electrical sparks. This electrical sparks are the result of discontinuity of over voltage produced due to quick rupture in the leakage current.

## IV. RESULTS AND DISCUSSION

### 4.1 X-ray Diffraction (XRD) of pristine GNPs and the nanocomposite:

XRD is a useful technique to find out the compatibility of the nanofiller with the blend while preparing the nanocomposite. XRD patterns of the GNPs and UPE/ESOA (80:20w/w)/GNPs nano composite with varying content of the nano filler are represented in Fig. 2. The GNPs exhibits a sharp peak at  $2\theta = 26.4^\circ$ , assigned to the stacking of the single graphene layers at a distance of 0.34 nm [13]. From Fig. 2A, for pristine GNPs no additional peak is observed. The XRD patterns of UPE/ESOA (80:20w/w) blend and UPE/ESOA (80:20w/w)/GNPs (1, 3, 5 wt %) nano composite show a primary broad peak of UPE resin at  $2\theta = 20^\circ$ . As Fig. 2B depicted the peak for the blend, so GNPs peak is absent here. Nanocomposite with 1 wt% nanofiller also shows no peak due to the diminutive concentration of GNPs that prevents systematic distribution of the nano filler (Fig. 2 C). The peak of GNPs at  $26.4^\circ$  start reappears with higher intensity at 3 wt% loading showing the preliminary phase of distribution of the nano filler. The highest intensity recorded at 5wt% of GNPs loading may be due to the presence of maximum amount of nanofiller in the nanocomposite. Similar results have been previously reported and the peak observed with reduced intensity was associated to the lower number of GNPs [14].

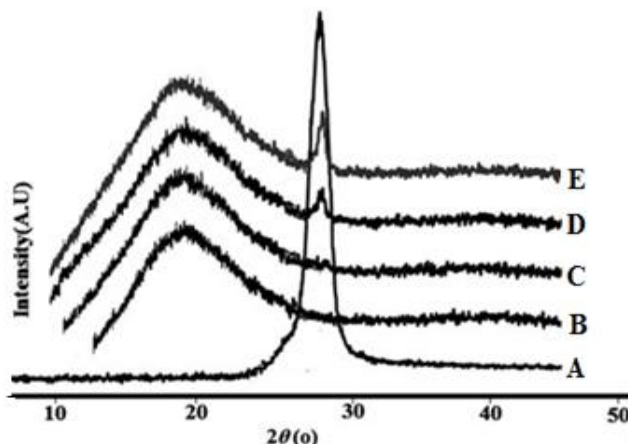


Fig. 2 XRD patterns of (A)GNPs,(B )UPE/ESOA(80:20) and (C)UPE/ESOA/GNPs (1wt%),(D)UPE/ESOA/GNPs (3wt%),(E)UPE/ESOA/GNPs (5 wt%)nanocomposites

### 4.2 Fourier transforms infrared (FTIR) spectroscopy:

Fig.3 shows the FTIR spectra of (A) GNPs

(B) UPE/ESOA (80:20w/w)/3wt% GNPs nanocomposites. The spectrum of GNPs shows a broad band at  $3450\text{ cm}^{-1}$  ascribing to the  $-\text{OH}_{\text{str}}$  group present in the GNPs. In Fig.3 B the characteristic peak at  $1618\text{ cm}^{-1}$  corresponds to the  $\text{C}=\text{C}_{\text{str}}$  from the GNPs. Again, the peak at  $1730$  and  $1752\text{ cm}^{-1}$  indicated the existence of  $\text{C}=\text{O}_{\text{str}}$  vibrations of the COOH group in GNPs and C-O-C groups in UPE respectively.

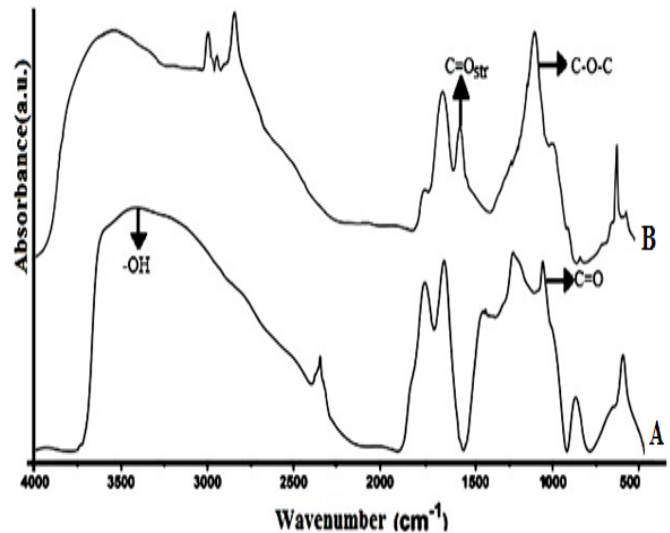


Fig. 3 FTIR of (A) pristine GNPs and (B) UPE/ESOA/GNPs nanocomposite.

The prominent absorption peak at  $1736\text{ cm}^{-1}$  attributes the presence of the formation of the ester group with the carboxyl of GNPs. The C-O-C groups from GNPs/UPE composite exhibit strong bands at  $1052\text{ cm}^{-1}$  confirms the occurrence of reaction between the carboxyl groups of UPE with the hydroxyl group of GNPs for the formation of nanocomposites.

### 4.3 Mechanical testing:

#### 4.3.1) Tensile properties:

Table 1 demonstrate the Tensile properties of the UPE/ESOA (80:20w/w)/GNPs nanocomposites containing varying contents of GNPs. GNPs loading have a tremendous effect on tensile strength of the nano composite. Strong interfacial interaction between the GNPs and the polymer matrix due to better dispersion of the nano filler enhances the homogeneity as well as mechanical properties of the composite. Tensile strength of UPE/ESOA (80:20w/w) blend improves as GNPs loading increases and attains the utmost value (51MPa) at 3wt% GNPs content. At 1 wt% of GNPs loading, the reinforcement effect is limited due to the low dispersion density of the filler. For 3wt% GNPs loading, the distribution and dispersion started to progress as the nanofiller concentration becomes greater for acting as a support to resist

maximum part of the load through effective interfacial stress transfer. Therefore, the tensile results imply better strength compared to 1 wt% GNPs loading. Further increase of nanofiller loading, decreases the tensile strength due to the agglomeration of the nano filler and uneven distribution in the blend. When the amount of GNPs reaches a critical content (5 wt %) and the distance between two GNPs is so small that they may be apt to stack together easily due to Van der Waals forces [15], thus it decreases the tensile strength. Tensile modulus is a common method to measure the stiffness of a material [16]. If tensile modulus enhances then the material was considered as rigid. Again table 1 shows tensile modulus of UPE/ESOA/GNPs nanocomposites. UPE/ESOA blend exhibited a tensile modulus value of  $3.7\text{GP}_a$  which increases to  $5.9\text{GP}_a$  on addition of 3wt% of GNPs. It may be due to the above said reasons.

Table 1 Mechanical properties of different types of nanocomposites.

Samples (GNPs loading) (Wt %)	Tenile strength ( $\text{MP}_a$ )	Tensile modulus ( $\text{GP}_a$ )	Bending strength ( $\text{MP}_a$ )	Bending modulus ( $\text{GP}_a$ )	Impact strength (J/m)	Fracture strain (%)
0	$37\pm 1$	$3.7\pm 0.2$	$44\pm 2$	$1.5\pm 0.1$	$48\pm 3$	$4.1\pm 3$
1	$42\pm 3$	$4.1\pm 0.3$	$49\pm 3$	$2.1\pm 0.2$	$52\pm 2$	$3.67\pm 1$
3	$51\pm 2$	$5.9\pm 0.2$	$55\pm 4$	$3.7\pm 0.1$	$67\pm 4$	$2.8\pm 2$
5	$47\pm 2$	$4.6\pm 0.2$	$42\pm 3$	$2.5\pm 0.1$	$58\pm 4$	$3.9\pm 3$

**4.3.2) Bending strength, bending modulus and impact strength:** The positive outcome of GNPs loading on the bending strength, bending modulus and impact strength of UPE/ESOA (80:20 w/w) nano composite are presented in table 1. The results suggested an increase in the properties at the nano filler concentration up to 3wt% due to better reinforcement effect of the nanofiller. This tendency confirms that interfacial interactions between the polymer and the nanofiller play vital role for determining the reinforcement efficiency in the nanocomposite. All these values reduce with increasing the nanofiller content up to 5 wt% owing to the formation of big clusters by the agglomeration of the GNPs. This leads to inhomogeneous dispersion in the polymer matrix and decreases the required properties. Actually proper distribution of GNPs reduces the chain flexibility of the blend by improving the cross linking density and enhances the stiffness.

**4.3.3) Fracture strain:** At 3wt% of GNPs nano filler lowest value of fracture strain is observed as the brittleness of the nano composite gradually decreased with the addition of this nanofiller. Further addition of nanofiller increases the value as the brittleness increases. This value is necessary as fracture strain. As it is the inverse of tensile modulus. Table 1 shows the fracture strain % of UPE/ESOA (80/20) blend with varying content of GNPs nano composite.

**4.3.4) Scanning electron microscopy (SEM):** Fig.4 shows the morphological structure analysis of (A) UPE/ESOA/GNPs

(1wt %) (B) UPE/ESOA/GNPs (3wt %) (C) UPE/ESOA/GNPs (5wt %) nanocomposites. As previously reported the blend without filler has relatively smooth and rubbery like elastic surface [8]. The UPE/ESOA/GNPs (1wt %) nanocomposite reveals less nanofillers dispersion in the matrix given in Fig. 4 A.

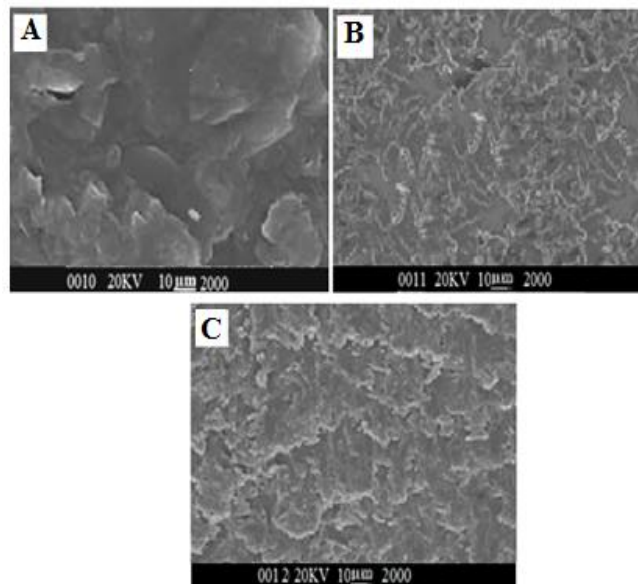


Fig. 4 SEM image of (A) UPE/ESOA/GNPs (1wt %)( B) UPE/ESOA/GNPs (3wt %) (C)UPE/ESOA/GNPs (5wt %) nanocomposite

3wt% filler in Fig. 4B shows rough but regular surface with the phase having homogeneity and good uniformity of the nano filler. It can be seen from this image that the GNPs filler was completely covered by the matrix phase, indicating a good adhesion between the all the phases. Better distribution of nano fillers enhances the properties and applicability of a composite. So this composition gave overall better properties.

Fig.4C depicts the SEM image of 5wt% of GNPs reinforced nanocomposites. Here agglomeration of the nanofiller occurs due to poor dispersability and improper orientation of the GNPs. This reduces the interfacial attraction between the blend and the nanofiller.

**4.3.5) Dynamic mechanical thermal properties:** Fig.5 shows the dynamic mechanical spectra in the form of storage modulus and loss factor ( $\tan\delta$ ) change with temperature for the nanocomposite with varying content of GNPs nanofiller loading. This DMA property of the UPE/ESOA blend has already reported in our earlier study [8]. The improvement in this property for nanocomposites in comparison to the blend may be due to better reinforcement of nanofiller and the restricted movement of the polymer chains caused by the chain confinement effect of the GNPs. The nanocomposites also showed higher glass transition temperature ( $T_g$ ) than the neat blend that suggested improved cross linking density and more crystallinity of the nanocomposite. This tendency enhances its capacity to take in a vibration and can scatter it all through the material without any failure. Moreover, at 3

Wt% nanofiller content the values of storage modulus and  $T_g$  attain utmost value with diminished loss modulus ( $\tan\delta$ ) due to proper orientation, strong interaction of nanofiller, reduced availability of free space in the nanocomposite, which made more energy requirement for the polymers during damping. Again at highest GNPs concentration of 5Wt% due to the clustering of nanofiller, there is availability of vacant space increases leading to slightly decreased cross linking density and increased polymeric chain flexibility.

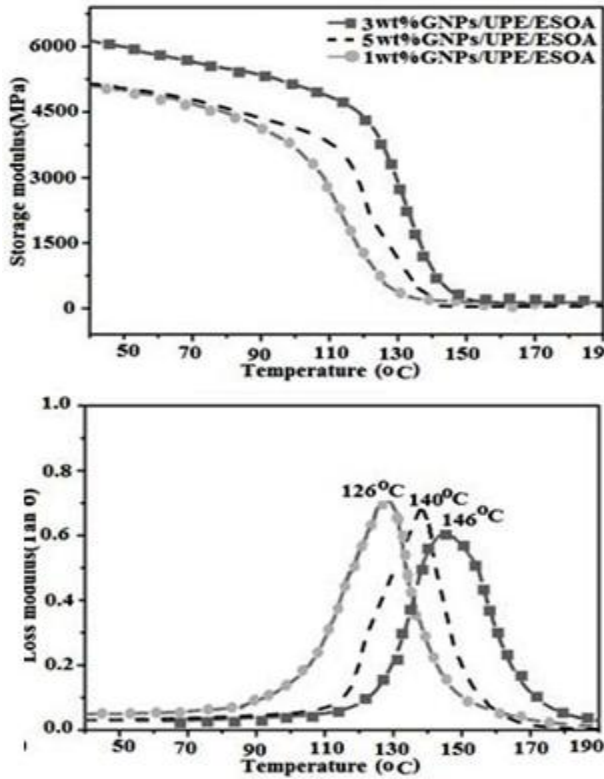


Fig.5: Dynamic mechanical spectra of different types of nanocomposites.

This tendency may cause the free movement of each polymer molecules due to low energy absorption capacity. So, here the storage modulus value decreases and damping coefficient value increases.

4.3.6) Differential Scanning Calorimetry:

The DSC result given in Fig.6, shows the variation of  $T_g$ s of the nanocomposites approached to higher temperature with the addition of nanofiller that was consistent with the DMA data given in Fig.5. It can be explained by two factors. First of all, the nanofillers restricted the movement of polymeric molecules due to formation of physical interlocking points in the blend. Secondly, GNPs created a strong bonding by reacting with the blend leading to enhanced cross linking density and crystallinity. Furthermore, 3Wt% of nanofiller content showed commendably efficient properties due to better dispersion of nanofiller. Again 5Wt% of GNPs showed decreased  $T_g$  due to poor dispersion and lower crystallinity.

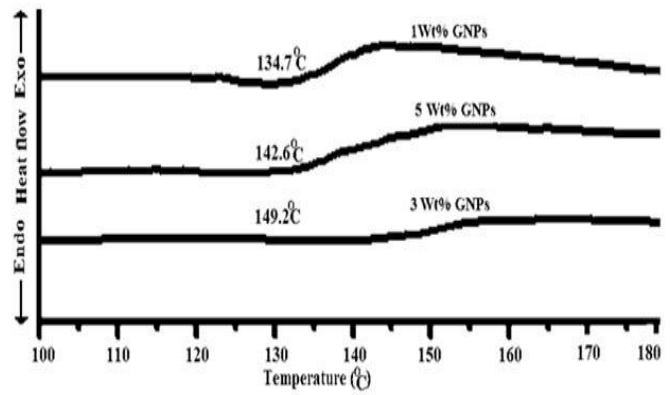


Fig.6: DSC of different types of nanocomposites

4.3.7) Surface resistivity:

Fig.7 represents the surface resistivity results, plotted as the effect of GNPs nanofiller loading on the UPE/ESOA nanocomposite. Actually this particular property of a material represents the electrical opposition of the surface of an insulating material towards leakage current. Here, the value decreases with increase in the concentration of the nanofiller. Lowest value of surface resistivity and highest value of surface conductivity was observed for 3 Wt% of GNPs loading. It may be

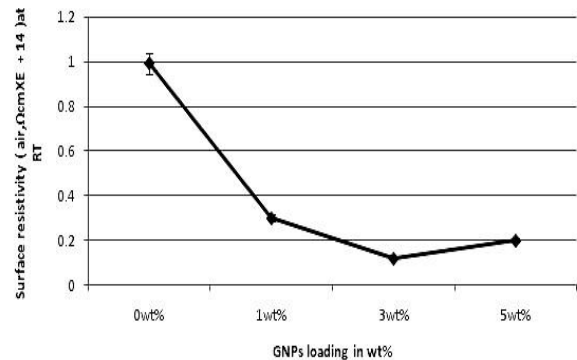


Fig.7: Surface Resistivity of UPE/ESOA blend and different types of nanocomposites.

due to the large surface area and platelet structure of the GNPs which created a large free path inside the polymer matrix for the propagation of free electron. It was observed that at higher loading of 5Wt% of GNPs content the filler particles tend to come closer due to the aggregation of matrix-filler interface which creates a barrier for conduction of electricity [17]. Moreover, this value varies in between  $0.97E+15 \Omega\text{-cm}$  to  $0.20E+15 \Omega\text{-cm}$  from 0 to 5Wt% of nanofiller loading.

4.3.8) Comparative tracking index:

Fig.8 represents an improvement of this above property of the nanocomposites by the introduction of nanofiller loading up to 3Wt%, after that the value diminished. At this concentration of GNPs, the nanocomposite demonstrated the highest value

as compared to the pristine UPE/ESOA blend as well as 1Wt% nanofiller content. It may be due to the better adhesion and dispersion ability of the nanofiller with the blend. Moreover, the nanocomposite with this particular concentration is also performing enormously high opposition to the alkaline surroundings. This tendency enhanced the capacity of the nanocomposite to bear up maximum arc voltage produced through the existence of moisture on the interface of the substrate.

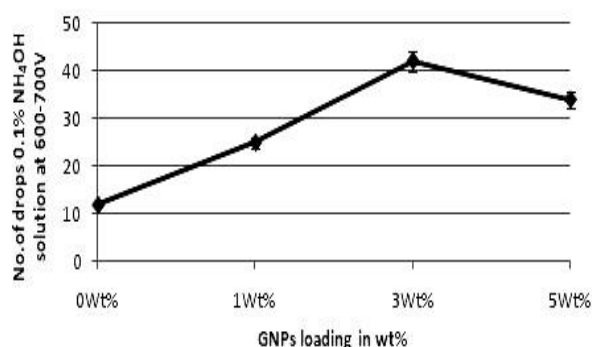


Fig.8: CTI of UPE/ESOA blend and different types of nanocomposites.

So the optimum properties are achieved at 3wt%. But at higher nanofiller content of 5 Wt%, large amount of agglomeration are observed that make the filler particles to get nearer to each other. This property may produce a strong obstacle for overall properties.

4.3.9) *Dry arc resistance*: Fig.9 presents the difference in resistance to high voltage arcing ignited on the sample surface with different concentration of GNPs loading for various arcing time. Voltage breakdown is characterized by carbonization of the conductive surface. Optimum voltage arc resistance capacity of 80 seconds was observed at 3wt% concentration of GNPs in UPE/ESOA nanocomposite whereas pristine UPE/ESOA blend showed 63 seconds of arc withstands.

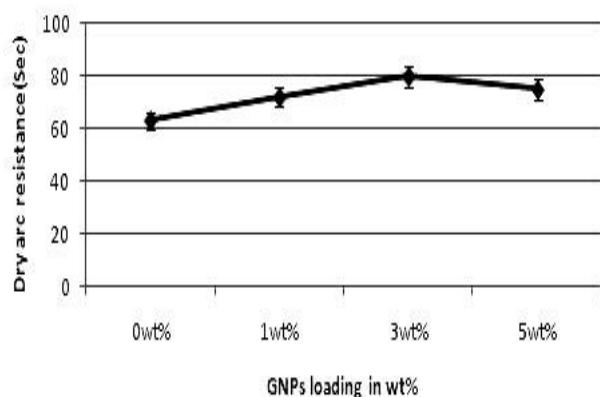


Fig.9: Dry arc resistance of UPE/ESOA blend and nanocomposites.

Increase in the property was observed up to 3wt% due to quasi dimensional and platelet structure of GNPs. This enhanced the compatibility between the blend and nanofiller which lead to the formation of best nanocomposite. After this particular concentration the dry arc resistance goes down due to clustering of nanofiller in the blend.

## V. CONCLUSION

The uniqueness of this work includes the use of Graphene nano platelets as nanofiller in varying proportions for the first time into UPE/ESOA (80:20) blend matrix. The overall results showed from XRD, SEM and FTIR that they have compatibility with possibility of co-reaction. The produced material has received much concentration due to their prospective to gain properties superior to conventional engineering materials. The studies revealed significant improvement in morphological, mechanical, dynamic mechanical, thermal and electrical properties which is very much important for various engineering and nanoelectronics applications. Effective stress transfer, reduced formation of flaws, slowed growth of microcracks and dissipation of extra mechanical energy resulting from efficient hybrid network in optimum concentration of 3wt% nanofiller were the reason behind this enhanced mechanical properties of this partly bio-nanomaterial. The successful increase in  $T_g$  to 149.2°C for 3wt% of GNPs content proved the superior confinement effect of the nanofiller with the blend. The optimum properties are achieved at 3wt% because at higher nano filler content of 5wt% the agglomeration of fillers has occurred that work as stress concentrators and reduce the overall properties. Again increment of cross linking density and crystallinity of the nano composite than the blend enhances their potential for application. Thus, the above nano composite could be a better candidate for a variety of structural applications with the ability of advanced functioning.

## ACKNOWLEDGEMENT

The authors of this paper are thankful to KIIT University for their support and help. The assistance provided by NIT, Rourkela and IIT, Kharagpur during the completion of the experimental works are greatly acknowledged.

## REFERENCES

- [1]. Singh, K., Ohlan, A., Dhawan, S. K., (2012). Polymer-Graphene Nanocomposites: Preparation, Characterization, Properties, and Applications. 3<sup>rd</sup> Chapt: INTECH.
- [2]. Potts, J. R., Dreyer, D. R., Bielawski, C. W., Ruoff, R. S., (2011) Graphene-based polymer nanocomposites. *Polym. Jan*7; 52(1): 5–25.
- [3]. Khot, S.N., Lascala, J.J., Can, E., Morje, S.S., Williams. G.I., Palmese. G.R., Kusefoglu, S.H., Wool. R.P. (2001)Development and application of triglyceride based polymers and composites. *J.Appl.Polym.Sci. Aug*13; 82(3):703-723.
- [4]. Raquez, J.M., Deléglise, M., Lacrampe, M.F., Krawczak. P. (2010)Thermosetting (bio) materials derived from renewable resources: A critical review. *Prog. Polym. Sci. Mar*; 35(4): 487-509.
- [5]. LaScala, J., Wool, R. P. (2005) Property analysis of triglyceride-based thermosets. *Polym. Jan*; 46(1): 61-69.

- [6]. Fu, L., Yang, L., Dai, C., Zhao, C., Ma, L. (2010) Thermal and mechanical properties of acrylated epoxidized-soybean oil-based thermosets. *J. Appl. Polym. Sci.* Aug13; 117(4): 2220-2225.
- [7]. Behera, D., Banthia, A.K. (2008) Synthesis, characterization and kinetics study of thermal decomposition of epoxidised soybean oil acrylate (ESOA). *J. Appl. Polym. Sci.* May9; 109(4): 2583-2590.
- [8]. Panda, S. K., Mohanty, P., Behera, D., Bastia, T. K. (2016) ESOA modified unsaturated polyester hybrid networks: A new perspective. *J. Appl. Polym. Sci.*, Sept6; 133(48). Available from: <http://onlinelibrary.wiley.com/doi/10.1002/app.v133.48/issueoc> doi: 11002/APP.44345.
- [9]. Zandiatashbar, A., Picu, R.C., Koratkar, N. (2012) Mechanical behavior of epoxy-graphene platelets Nanocomposites. *J. Eng. Mater. Technol.* May; 134(3): 031011–031016.
- [10]. Yang, S. Y., Lin, W. N., Huang, Y. L., Tien, H. W., Wang, J. Y., Ma, C. C., Li, S. M. (2011) Synergetic effects of graphene platelets and carbon nanotubes on the mechanical and thermal properties of epoxy composites. *Carbon.* Mar; 49(3): 793–803.
- [11]. Ahmadi-Moghadam, B., Taheri, F. (2014) Effect of processing parameters on the structure and multi-functional performance of epoxy/GNPS-nanocomposite. *J. Mater. Sci.* Jun10; 49(18):6180–6190.
- [12]. Li, W., Dichiaro, A., Bai, J. (2012) Carbon nanotube-graphene nanoplatelet hybrids as high-performance multifunctional reinforcements in epoxy composites. *Compos. Sci. Technol.* Dec 6; 74: 221–227.
- [13]. Causin, V., Marega, C., Marigo, A., Ferrara, G., Ferraro, A. (2006) Morphological and structural characterization of polypropylene /conductive graphite nanocomposites. *Eur. Polym. J.* Jun; 42(12), 3153–3161.
- [14]. Yasmin, A., Luo, J.J., Daniel, I. M. (2006) Processing of expanded graphite reinforced polymer Nanocomposites. *Compos. Sci. Technol.* Nov; 66(9):1182–1189.
- [15]. Zhao, X., Zhang, Q., Chen, D., Lu, P. (2010) Enhanced mechanical properties of graphene-based poly(vinyl alcohol) composites. *Macromolecules.* Feb9; 43(5):2357–2363.
- [16]. Finkenstadt, V., Liu, C. K., Cooke, P., Liu, L., Willett, J. (2008) Mechanical property characterization of plasticized sugar beet pulp and poly(lactic acid) green composites using acoustic emission and confocal microscopy. *J. Polym. Environ.* Jan; 16(1): 19–26.
- [17]. Wang, Z., Nelson, J.K., Miao, J., Linhardt, R.J., Schadler, L.S., Hillborg, H., Zhao, S. (2013) Dielectric constant and breakdown strength of polymer composites with high aspect-ratio fillers studied by finite element models. *Compos. Sci. Technol.* Mar; 76:960–6.